THE JOURNAL OF BIOLOGICAL CHEMISTRY
Vol. 280, No. 18, Issue of May 6, pp. 18042–18048, 2005
Printed in U.S.A.

Increased Flexibility as a Strategy for Cold Adaptation

A COMPARATIVE MOLECULAR DYNAMICS STUDY OF COLD- AND WARM-ACTIVE URACIL DNA GLYCOSYLASE*

Received for publication, January 26, 2005, and in revised form, March 3, 2005
Published, JBC Papers in Press, March 3, 2005, DOI 10.1074/jbc.M500948200

Magne Olufsen, Arne O. Smalås, Elin Moe, and Bjørn O. Brandsdal‡

From The Norwegian Structural Biology Centre, University of Tromsø, N-9037 Tromsø, Norway

Uracil DNA glycosylase (UDG) is a DNA repair enzyme in the base excision repair pathway and removes uracil from the DNA strand. Atlantic cod UDG (cUDG), which is a cold-adapted enzyme, has been found to be up to 10 times more catalytically active in the temperature range 15–37 °C as compared with the warm-active human counterpart. The increased catalytic activity of cold-adapted enzymes as compared with their mesophilic homologues are partly believed to be caused by an increase in the structural flexibility. However, no direct experimental evidence supports the proposal of increased flexibility of cold-adapted enzymes. We have used molecular dynamics simulations to gain insight into the structural flexibility of UDG. The results from these simulations show that an important loop involved in DNA recognition (the Leu^{272} loop) is the most flexible part of the cUDG structure and that the human counterpart has much lower flexibility in the Leu^{272} loop. The flexibility in this loop correlates well with the experimental k_{cat}/K_m values. Thus, the data presented here add strong support to the idea that flexibility plays a central role in adaptation to cold environments.

A vast amount of our planet consists of cold environments, like the Arctic, Antarctic, mountain regions, and deep sea waters, and cold-adapted organisms are able to breed and grow successfully in these regions. Organisms that are adapted to these extreme environments are often termed psychrophiles, whereas their warm-active counterparts are referred to as mesophiles and thermophiles. The temperature is one of the most important factors for enzyme activity, and enzymatic reaction rates can be reduced 30–80 times when the temperature decreases from 37 to 0 °C (1). To deal with this strong temperature dependence, cold-adapted enzymes usually have higher catalytic activity at low temperatures and decreased thermostability as compared with their mesophilic and thermophilic counterparts (1). Several strategies have been postulated to explain how enzymes adapt to cold environments, and the main theory, although not proven, has been that increased structural flexibility in psychrophilic enzymes enhances the catalytic efficiency (2). It is not necessarily that the elevated flexibility is attributed to an overall increase but may equally well be a result of increased flexibility for some of the structural elements. Improved flexibility in local areas seems to be a strategy for cold-adapted enzymes to maintain high catalytic activity at lower temperatures (3–5). Increased flexibility of psychrophilic enzymes would also explain the observed decrease in thermal stability (5). The observed increased catalytic activity at low temperatures and the decreased thermostability of psychrophilic enzymes suggest that there is a relationship between stability and activity to maintain the activity at low temperatures. The stabilizing intramolecular forces are consequently weakened, giving rise to a reduction in the thermal stability (6). The stability/flexibility relationship is controversial because cold-adapted organisms are under no selective pressure to stabilize proteins at elevated temperatures, and it is believed that the stability property has slowly vanished due to genetic drift (7).

Enzymes use different strategies to adopt to cold environments. Several cold-adapted enzymes studied so far seem to have low relative arginine content (Arg/(Arg+Lys)) as compared with the mesophilic and thermophilic enzymes (8). A decreased number of proline residues and an increased number of glycine residues are also thought to be a strategy that cold-adopted enzymes use (9). Another difference is that cold-adapted enzymes in some cases have a lower content of ion pairs, aromatic interactions, and/or hydrogen bonds (6). The above mentioned factors may give rise to increased local or overall molecular flexibility.

Although the flexibility hypothesis has been the dominating theory to explain the increased catalytic efficiency of cold-adapted enzymes, other adaptational strategies should not be ruled out. Optimization of the electrostatic potential is of great importance for the higher catalytic efficiency for cold-adapted enzymes (10). The increased binding affinity observed for the cold-adapted anionic salmon trypsin as compared with the mesophilic bovine trypsin is caused by optimization of electrostatic features (11). In the cod uracil DNA glycosylase (cUDG)[1], there are data supporting that the cold-adapted features observed could be caused by optimization of the electrostatic surface potential (12).

Uracil DNA glycosylase (UDG) is a DNA repair enzyme and is involved in the base excision repair pathway removing uracil from the DNA stand (13). This enzyme, which is the first in the base excision repair pathway, catalyzes the hydrolysis of promutagenic uracil residues from single- or double-stranded DNA. The crystal structure of the catalytic domain of UDG from several species are known: human (hUDG) (14), cod (cUDG) (15), virus 1 (16), and *Escherichia coli* (17). The three-dimensional structure of UDG in complex with DNA has also been determined (16, 18–21). Cold-adapted cUDG has been found to be up to 10 times more catalytic efficient (k_{cat}/K_m) in the temperature range 15–37 °C as compared with the human

* The costs of publication of this article were defrayed in part by the payment of page charges. This article must therefore be hereby marked "*advertisement*" in accordance with 18 U.S.C. Section 1734 solely to indicate this fact.

‡ To whom correspondence should be addressed. Tel.: 47-77644057; Fax: 47-77644765; E-mail: Bjorn-Olav.Brandsdal@chem.uit.no.

[1] The abbreviations used are: UDG, uracil DNA glycosylase; cUDG, cod UDG; hUDG, human UDG; r.m.s.d., root mean square deviation; MD, molecular dynamics.

counterpart (22). cUDG is also found to be less stable than hUDG at all temperatures examined (23). The catalytic domain of hUDG and cUDG consists of 223 amino acids, and the sequence identity between them is 75%. The overall topology is a typical α/β protein (14). The loops involved in detection and catalysis of uracil are conserved in cUDG and hUDG, and the loops important to catalysis are: 4-Pro loop (^{165}PPPPS^{169}), the Gly-Ser loop (^{246}GS^{247}), the Leu^{272} loop (^{268}HPSPLSVYR^{276}), and the water-activating loop (^{145}DPYH^{148}) (20). The amino acids mentioned above are from hUDG, and there are two substitutions in the Leu^{272} loop in the cUDG structure: V274A and Y275H. The Leu^{272} loop is an important loop as it moves into the minor groove of the double-stranded DNA and flips out the uracil base. This movement is essential for bringing the catalytic important residue, His^{268}, within hydrogen-bonding distance of uracil (the O_2 atom) (20).

Visualization of the electrostatic potential of cUDG and hUDG indicated that the former has a more positively charged surface near the active site. The amino acids at positions 171 and 275 seem to be two key residues when explaining the difference in the surface potential (15, 24). Several mutants were subsequently constructed and analyzed in terms of kinetic, thermodynamic, and structural properties (12, 15, 24). In this study, molecular dynamics (MD) simulations have been performed for six UDG variants and were also repeated with DNA bound. The UDG variants included are: cUDG, cUDG-H275Y, cUDG-V171E, and cUDG-loop (A266T, V267A, A274V and H275Y) and hUDG and hUDG-E171V. It has previously been suggested that differences in catalytic activity could be explained by flexibility in the Leu^{272} loop area (15), and in this report, the relationship between the flexibility and catalytic activity is studied by means of MD simulations. The emerged picture is that cold-adapted enzymes have higher flexibility in the catalytic important areas of the structure (6). However, no direct experimental evidence supporting the hypothesis of increased flexibility of cold-adapted enzymes has yet been provided. MD simulations can provide insight into the dynamics of proteins and have been used to study the structural flexibility of UDG homologues.

MATERIALS AND METHODS

Models—Crystal structures were available for all of the UDG variants, except the cUDG-H275Y and the cUDG-loop mutant, and in the latter cases, models were made in the O program (25) from the cUDG structure. These structures were used as starting structures in the MD simulations. All the crystal structures were recombinant enzymes with three mutations in the N-terminal end: P82M, V83E, and G84F. The crystal structure of UDG in complex with double-stranded DNA (Protein Data Bank entry: 1EMH) (19), consisting of 19 bases, was used as a starting structure for the hUDG-DNA simulation and as a template to model the other complexes. This DNA originally had a 2′-deoxypseudouridine-5′monophosphate but was modeled into a 2′-deoxy-uracil-5′monophosphate by switching the places of the atoms: C2 ↔ C4, O_2 ↔ O4 and N1 ↔ C5 (Fig. 1). The latter is the uracil base that UDG recognizes and removes from the DNA strain.

UDG contains several histidines, and these were considered as neutral in the simulations, except for His^{148}. These choices were based on data from NMR and continuum electrostatics calculations (26). The hydrogen-bonding pattern of all histidines was analyzed to determine the position of the proton, and the proton was placed on the Nδ atom on the neutral histidines.

Molecular Dynamics—The AMBER program package (27) and the AMBER95 force field (28) were used to run and analyze all the MD simulations. The systems were energy-minimized by 2000 steps of steepest decent followed by 3000 steps using the conjugate gradients method. In the initial phase, the temperature of the system was slowly raised in steps to the final temperature of 300 K followed by an equilibration period of 50 ps. The time step used was 2 fs. In the production phase, the simulation was run with the isothermal-isobaric ensemble (300 K and one atmosphere pressure), and pressure and temperature were maintained by the Berendsen coupling algorithm (29). A 10 Å cutoff for non-bonded interactions was used in the simulation, and the Particle-Mesh Ewald method (30) was used to handle long range interactions. The SHAKE procedure (31) was applied to restrain covalent bonds involving all hydrogen atoms. During the production phase, the coordinates were written to file every ps. Crystallographic waters were kept, and in addition, water molecules were added, according to the TIP3P model (32), around the protein with a 15 Å buffer from the edge of the periodic box. The total box size for the system was ~85 × 70 × 75 Å with roughly 50,000 atoms in the system. The simulations were run for 1 ns for each mutant except for native cUDG and hUDG, which were run for 2 ns. Average structures were calculated from the snapshots during the simulation. To examine the stability of the protein during the simulation, the root mean square deviation (r.m.s.d.) of Cα atoms *versus* simulation time was calculated. r.m.s.d. based on main chain atoms has also been calculated, but these values were very similar to the Cα r.m.s.d., and the Cα r.m.s.d. is therefore used throughout this text.

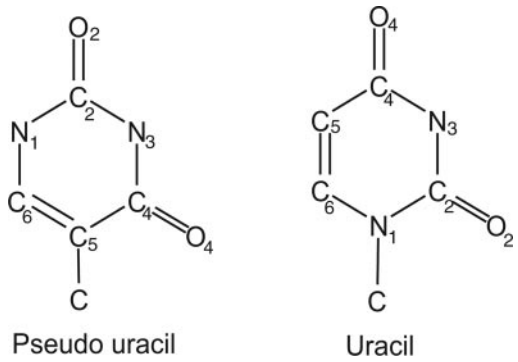

FIG. 1. **Structural differences between uracil and pseudo uracil.**

RESULTS AND DISCUSSION

Thermodynamic and kinetic characterizations of cUDG and hUDG have shown that the former is more catalytic efficient and less thermostable as compared with the latter. To gain insight into the features responsible for these properties, several mutants of cUDG and hUDG have been constructed and subsequently investigated by combining biochemical analysis with three-dimensional structure analysis (12, 15, 24). To gain further insights into the role that molecular flexibility plays in enzymatic adaptation to cold environments, six different UDG variants have been studied by MD simulations. The six different variants are: cUDG, cUDG-V171E, cUDG-H275Y, cUDG-loop mutant (A266T, V267A, A274V, and H275Y), hUDG, and hUDG-E171V. Fig. 2 shows cUDG bound to the DNA fragment with important residues highlighted. The variants studied have been mutated from the amino acid in native cUDG to the amino acid in native hUDG and vice versa. All of them have previously been characterized in terms of kinetics and thermodynamics, and K_m and k_{cat} values are available for each of them (Table I) (12).[2]

Analysis of the crystal structure of hUDG and hUDG in complex with DNA has shown that the Leu^{272} loop moves when the enzyme binds to the DNA strand. This movement is essential for bringing the catalytic His^{268} into hydrogen-bonding distance of the uracil O_2. Residues 275 and 276 in the Leu^{272} loop are involved in DNA repair recognition (20), and it is therefore reasonable to expect that this loop is very important for catalytic activity.

Overall Features of the MD Simulations—To assess the stability of the simulations, the r.m.s.d. has been calculated relative to the average structure (calculated from the coordinates from the production phase) and is presented in Fig. 3*A* for native cUDG and hUDG. Fig. 3*A* shows that the r.m.s.d. for the

[2] E. Moe, I. Leiros, K. Torseth, O. Lanes, A. O. Smalås, and N. P. Willassen, unpublished results.

FIG. 2. **A ribbon structure of the cUDG-DNA model used in the MD simulation.** Some residues are drawn in a *ball-and-stick*. The program DSSP (34) was used to find the secondary structure, and the figure was generated by Molscript (35) and Raster3D (33). *C-term*, C terminus.

TABLE I
Average r.m.s.d of Cα atoms after 1 ns of MD simulation and kinetic constants determined at 22 °C for cUDG, hUDG, and four mutants (Ref. 12 and Footnote 2)

UDG	r.ms.d.		k_{cat}/K_m	k_{cat}	K_m
	Average	Residues 268–276			
	Å		$min^{-1}\mu M^{-1}$	min^{-1}	μM
cUDG	0.62	1.38	892	677	0.8
cUDG-DNA	0.58	0.62			
cUDG-loop	0.58	1.04	548	263	0.5
cUDG-loop-DNA	0.52	0.50			
cUDG-H275Y	0.59	0.96	509	302	0.6
cUDG-H275Y-DNA	0.54	0.50			
hUDG-E171V	0.57	0.85	396	262	0.7
hUDG-E171V-DNA	0.48	0.44			
hUDG	0.55	0.97	135	320	2.4
hUDG-DNA	0.50	0.42			
cUDG-V171E	0.56	0.67	117	204	1.7
cUDG-V171E-DNA	0.49	0.54			

cold-adapted cUDG is between 0.5 and 1.3 Å during the simulation, whereas the hUDG simulations display lower overall r.m.s.d. In all 12 MD simulations, the total r.m.s.d. is stable through the simulation (results not shown).

There are only small differences in the average r.m.s.d. among the different UDG variants (Table I), calculated for 1000 MD structures. The UDG simulations without DNA have an r.m.s.d. between 0.56 and 0.62 Å, whereas the corresponding values for the simulations with DNA are between 0.48 and 0.58 Å (Table I). The cold-adapted cUDG has the highest average r.m.s.d., both with and without DNA bound, whereas the warm-active hUDG-E171V and hUDG-DNA display the lowest r.m.s.d. It is interesting to note that cUDG has the highest r.m.s.d. both when DNA is present and when DNA is absent as this indicates that the cold-active UDG has higher overall flexibility as compared with its warm-active counterpart hUDG. This is to our knowledge the first time MD simulations show that a cold-adapted enzyme has increased overall molecular flexibility as compared with its warm-active counterpart. However, based on this, one cannot conclude that the increased flexibility is the basis for the enhanced catalytic activity as observed experimentally, although strong evidence is presented. Comparison of the r.m.s.d. for the DNA recognition loop (Leu^{272} loop, residues 268–276) shows that there are large differences among the UDG variants, and this issue will be discussed in the next sections.

Comparison of Human and Cod UDG—To further investigate the details of the MD simulations, the average r.m.s.d.

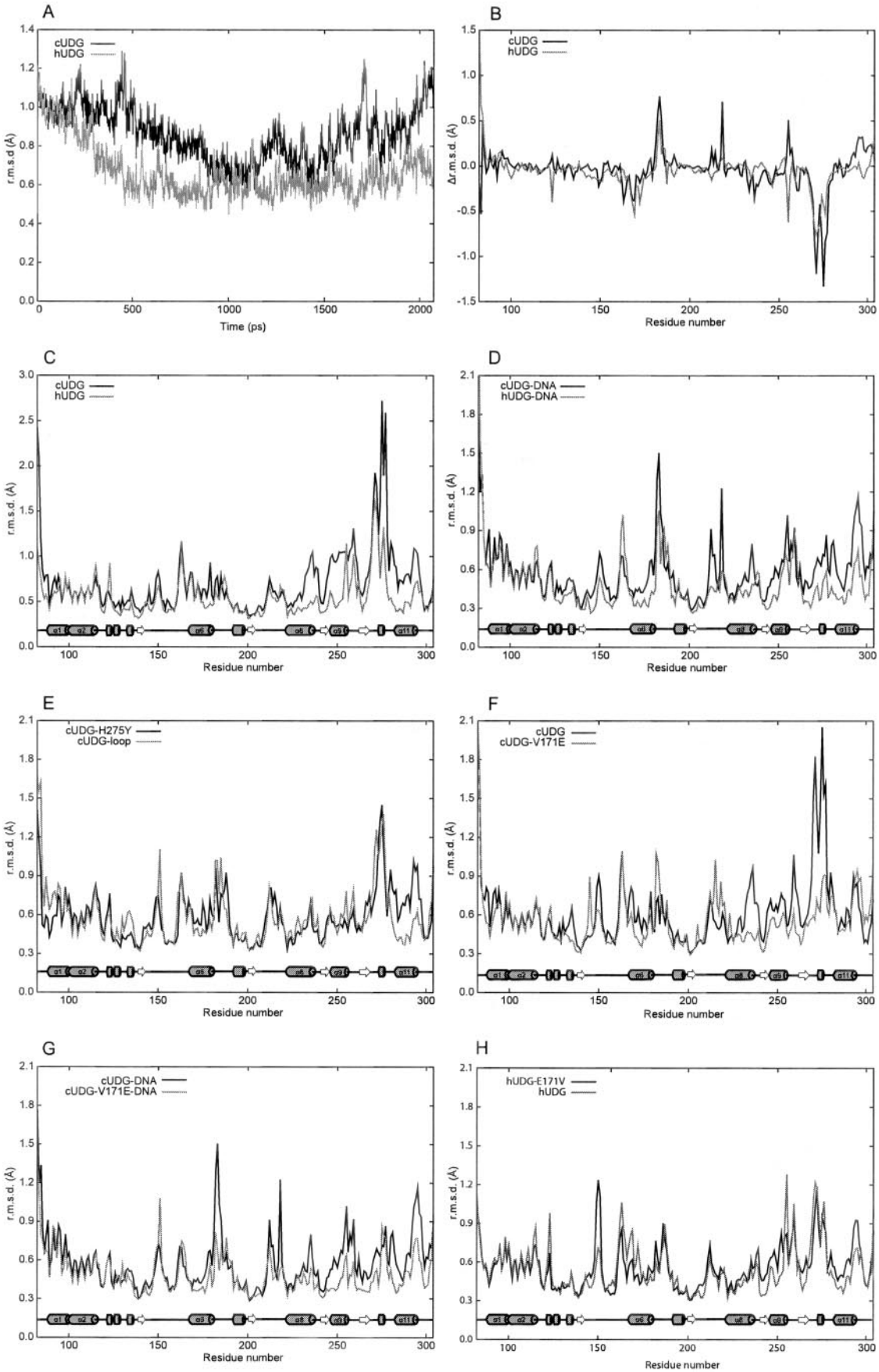

FIG. 3. **Various r.m.s.d. plots from the MD simulations.** *A*, a plot of the r.m.s.d. as a function of time for the simulation of hUDG and cUDG, calculated based on all Cα atoms in the average structure and the snapshot during the simulation. *B*, Δr.m.s.d. ($r.m.s.d._{UDG\text{-}DNA} - r.m.s.d._{UDG}$) per residue of cUDG and hUDG. *C*, r.m.s.d. of cUDG and hUDG calculated from 2 ns of MD simulation at 300 K. *D–H*, r.m.s.d. calculated from 1 ns of MD simulation at 300 K.

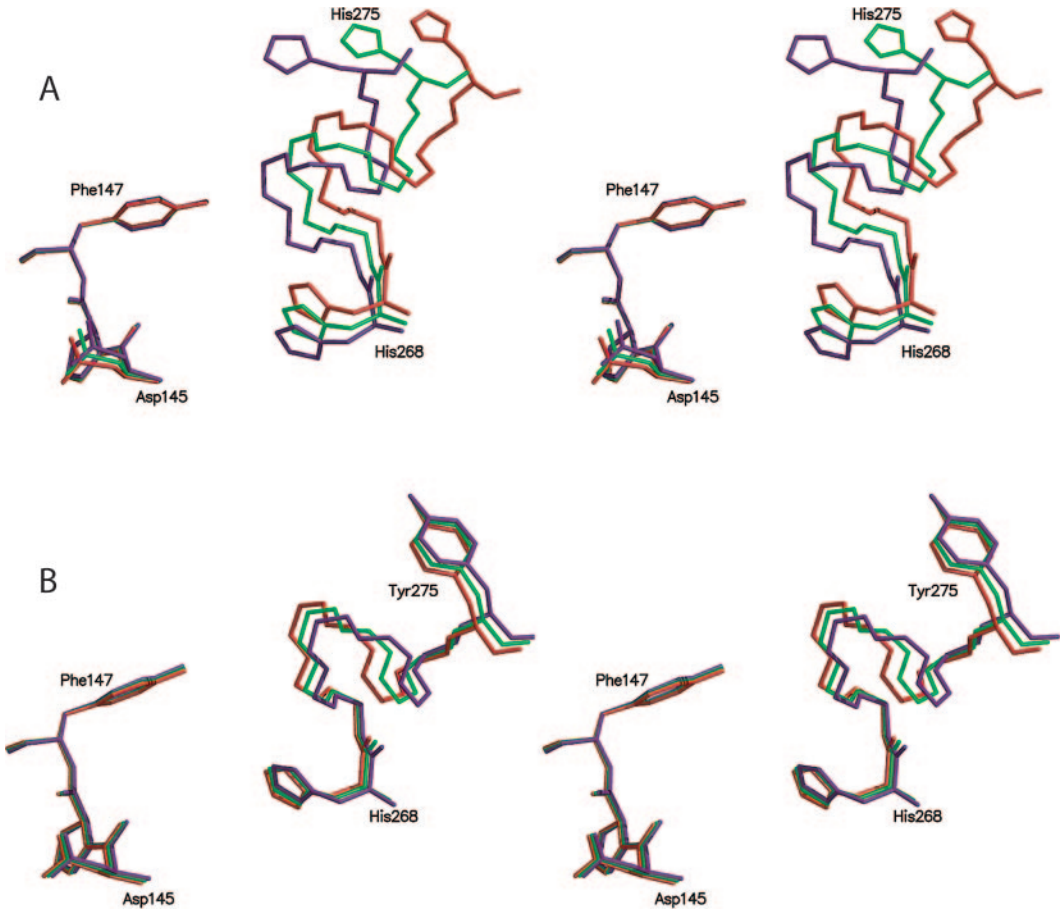

FIG. 4. **Movement of the DNA binding loop from the cUDG and hUDG simulations.** Average structures of the cUDG Leu^{272} loop (*A*) and hUDG Leu^{272} loop (*B*) from 0 to 1 ns (*red*), 0 to 2 ns (*green*), and 1 to 2 (*blue*) ns simulation has been superimposed. From residues 269 to 274, only main chain atoms are drawn, and residue 276 is not shown. The figures were generated by Molscript (35) and Raster3D (33).

values/residue for the simulations have been calculated. Fig. 3*C* shows a comparison of the average r.m.s.d. for the Cα atoms of cUDG and hUDG. Several large differences are observed in the C-terminal end of the protein, especially in the Leu^{272} loop. The residue with highest r.m.s.d. is also found in this region, which is His^{275} in the cUDG simulations and Pro^{271} in hUDG. The Gly-Ser loop (^{246}GS^{247}) is also more flexible for the cod variant with an increased r.m.s.d. of 0.41 Å relative to the human counterpart. Three average structures have been calculated from these two simulations based on the coordinates from 0 to 1, 0 to 2, and 1 to 2 ns of cUDG and hUDG. Analysis of these structures reveals that the Leu^{272} loop of the cod structure moves throughout the simulation (Fig. 4*A*). In contrast, the average structures from the hUDG simulation are much more similar, and consequently, less movement is observed in this loop region (Fig. 4*B*). For the cUDG simulation, the Cα atom in the His^{275} residue moves 5.47 Å from the initial to the final structure, whereas the same atom moves 4.83 Å between the average structure from 0 to 1 ns and the average structure from 1 to 2 ns simulation. During the hUDG simulation, this movement is not observed (Fig. 4, *A* and *B*). The crystal structures of cUDG and hUDG have approximately the same number of charged residues, but the cUDG structure was found to have slightly more hydrogen bonds (15). One should believe that the slight increase in hydrogen bonds in the cUDG structure would make the cUDG structure more rigid than the hUDG structure, but this does not seem to be the case according to the MD simulations.

In the simulations of cUDG and hUDG in complex with DNA, the structure of the former is again more flexible than the human counterpart, especially in the C-terminal part of the protein (Fig. 3*D*). The average residual r.m.s.d. decreases only by 0.04 and 0.05 Å between the unbound UDG simulation and the complex simulation of the cUDG and the hUDG, respectively. We have also calculated the Δr.m.s.d. (r.m.s.d.$_{\text{UDG-DNA}}$ − r.m.s.d.$_{\text{UDG}}$) to investigate the effect of DNA on the molecular flexibility. Fig. 3*B* shows that most of the flexibility is lost in the Leu^{272} loop area for both the cUDG and the hUDG structure. The decrease in flexibility in the Leu^{272} loop upon DNA binding is observed for all the different UDG variants. This loop is in close contact with the DNA, and it therefore seems reasonable that the r.m.s.d. in this area will decrease when DNA is included in the simulations. Around residue 183 (Gly for cUDG and Asp for hUDG), both structures have an increase in r.m.s.d. for the simulation of the complex; residue 183 is not close to the DNA or the DNA binding area but is situated at the outside of the protein. In the average structure of hUDG and hUDG-DNA, the Asp^{183} side chain forms a salt bridge to Lys^{302}, and the distance between the Nζ atom and the Oδ1 and Oδ2 is 2.76 and 3.36 Å in the hUDG and 2.93 and 3.25 Å in the hUDG-DNA structure. In the average structure of cUDG and cUDG-DNA, Gly^{183} does not form any interactions. Therefore, it is difficult to explain this increase in mobility for residue 183 in the complex simulation, but DNA is highly charged and may therefore influence all parts of the protein through long range interactions and changes in electrostatic potentials. This could affect the flexibility of the protein.

Analysis of the cUDG-Loop and the cUDG-H275Y Simulations—The cUDG-loop mutant (A266T, V267A, A274V, and H275Y) and the cUDG-H275Y mutant have similar k_{cat}/K_m values, 548 and 509 min$^{-1}\mu$M^{-1}, respectively, whereas the

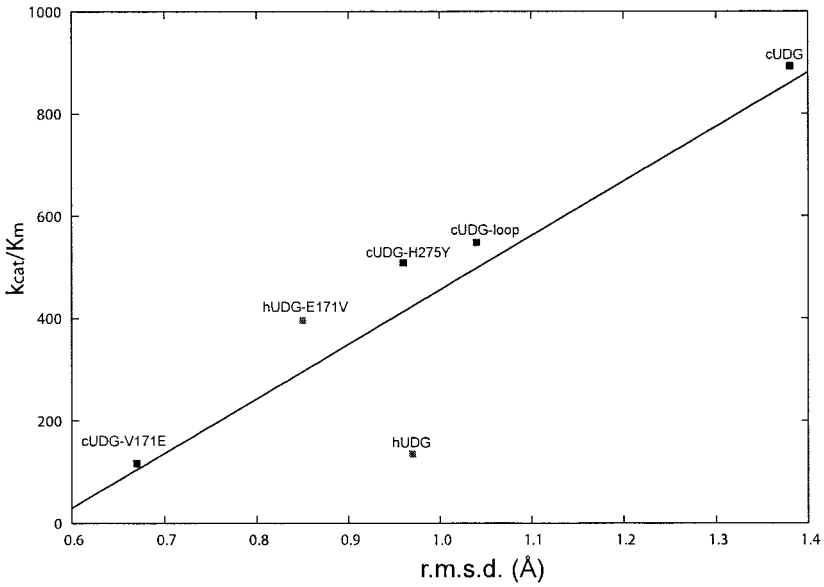

FIG. 5. **Plot of k_{cat}/K_m (catalytic efficiency) *versus* Cα r.m.s.d. of the Leu^{272} loop for the different UDG variants.**

native cod enzyme has a k_{cat}/K_m value of 892 $min^{-1}\mu M^{-1}$ (12). The average Cα r.m.s.d. values of the Leu^{272} loop are 1.04 and 0.96 Å for the cUDG-loop and cUDG-H275Y simulations, respectively, whereas the corresponding value for cUDG is 1.38 Å. Thus, the catalytic efficiency decreases with these substitutions, and there appears to be a concomitant decrease in the flexibility of the Leu^{272} loop for the MD simulations. It therefore seems likely that there is a close connection between the flexibility of the Leu^{272} loop and catalytic efficiency.

The nature of the amino acid at position 275 seems to be a key factor to explain the flexibility of the Leu^{272} loop. It is reasonable to expect that the difference in the side chain volume, size and charge can reduce the flexibility of this residue and subsequently the loop for hUDG. It is found that when mutating H275Y in cUDG, the r.m.s.d. for the Cα atom of residue 275 is reduced by 0.60 Å as compared with the cUDG simulation (Fig. 3, *C* and *E*). If we consider all the residues in the Leu^{272} loop, the r.m.s.d. of the cUDG-loop and the cUDG-H275Y simulations is virtually identical to that observed for hUDG (Fig. 3, *C* and *E*), which also indicates that the His to Tyr mutation is responsible for the decreased flexibility of this loop. It has been suggested that Val^{274}, Tyr^{275}, and Phe^{279} residues in the hUDG structure form a hydrophobic cluster and that this cluster will restrict the motion of the Leu^{272} loop. All three residues are substituted to smaller ones in the cUDG structure (Ala^{274}, His^{275}, and Leu^{279}) (15). The Cα r.m.s.d. of Pro^{271} decreases by 1.09 Å for the cUDG-H275Y average structure as compared with the average structure from the cUDG simulation. The carbonyl oxygen of residue Pro^{271} of cUDG-H275Y is involved in two hydrogen bonds to main chain nitrogens in residues 273 and 274 with a distance of 3.39 and 3.23 Å, respectively, whereas in the average structure of cUDG, the distances between the same atoms are 3.67 and 3.85 Å, respectively. This difference may explain why the native cUDG structure has a more flexible Pro^{271} residue.

Analysis of the cUDG-V171E and the hUDG-E171V Simulations—The residue at position 171 is important for the cold-adapted features of cUDG as k_{cat}/K_m decreases by almost a factor of 8 when Val^{171} is mutated to Glu, which is the amino acid in the mesophilic human sequence. The cUDG-V171E mutant also shows increased temperature stability at 37 °C as compared with cUDG (12). The Cα r.m.s.d. plot of the cUDG-V171E structure is quite different from the cUDG structure, especially in the Leu^{272} loop where the difference in r.m.s.d. is 0.71 Å (Fig. 3*F*). It is interesting to note that the mutation of the 171 residue does not have any effect on the flexibility of the nearby residues but does have a large effect on the residues in the Leu^{272} area. Moe *et al.* (12) have shown that the electrostatic environment near the catalytic region of the enzyme is of vital importance to the catalytic efficiency. Thus, it is likely that the change in electrostatic environment could explain why the 171 substitution has a large effect on the flexibility of the Leu^{272} loop. The r.m.s.d. values of both cUDG-V171E and cUDG in complex with DNA (Fig. 3*G*) show that the cUDG has higher flexibility in the Leu^{272} loop, but the largest differences in r.m.s.d. values between the two structures are for residues 182–185. The average structure of the cUDG-V171E-DNA has a weak salt bridge between the side chain of Glu^{171} and His^{186} (4.40 Å), which can explain the decrease in r.m.s.d. in the sequence 182–185.

The hUDG-E171V mutant has a 3-fold increased catalytic efficiency and also decreased temperature stability as compared with the native human enzyme (12); thus, substitution from an amino acid found in the warm-active enzyme to an amino acid in the cold-adapted cUDG makes the enzyme adopt the typical cold-adapted features. The hUDG-E171V mutant also has a lower flexibility in the Leu^{272} loop as compared with hUDG (Fig. 3*H*), whereas in the complex simulation, more or less the same flexibility is observed.

The cUDG-V171E variant has the lowest r.m.s.d. value in the Leu^{272} loop and also displays the lowest catalytic efficiency in the study, whereas both the k_{cat}/K_m and the r.m.s.d. of the Leu^{272} loop for the hUDG-E171V variant are in the middle between the endpoints drawn by native cUDG and cUDG-V171E. These results fit well with the idea that there is a correlation between catalytic efficiency and flexibility of this loop.

Concluding Remarks—MD simulations of UDG have been used to predict the flexible parts of the enzyme, and the Leu^{272} loop is the most mobile part of the structure for all of the UDG variants included in our study, except for the cUDG-V171E mutant, which has higher flexibility in other parts of the structure (Fig. 3, *C* and *E*–G). In addition, these simulations show that the C-terminal end of cUDG enzyme is more flexible as compared with the human counterpart, as postulated previously (22). The His^{275} residue in cUDG is probably the main contributor to the increased flexibility of the Leu^{272} loop, relative to the human enzyme. The size, volume, and charge of this residue can probably explain the increased flexibility of the Leu^{272} loop of the cod enzyme. Another interesting aspect is

that the r.m.s.d. of the Leu^{272} loop correlates well with the k_{cat}/K_m values as cUDG has by far the highest k_{cat}/K_m value and it also has by far the highest flexibility in the Leu^{272} loop, whereas the cUDG-V171E mutant has the lowest r.m.s.d. in the Leu^{272} loop and also the lowest k_{cat}/K_m of the mutants in this study. Five of the six r.m.s.d. values of the Leu^{272} loop from the UDG correlate with the k_{cat}/K_m values (Fig. 5); the correlation factor is 86.4% for all the variants and 99.0% if the outlier hUDG is excluded. In the UDG-DNA simulation, there is less difference in r.m.s.d. among the variants, but still, cUDG-DNA has the highest r.m.s.d. value, and the warm-active variant has the lowest r.m.s.d. values of the Leu^{272} loop. This verifies the hypothesis that states that cold-adapted enzymes are characterized by an improved flexibility of the structural components involved in the catalytic cycle (6) for UDG. By analysis of the activation parameters of cold-adapted enzymes, it has been shown that local flexibility is essential for high activity at low temperatures (1), and these findings fit well with the suggested link between catalytic efficiency and flexibility of the DNA recognition loop of UDG.

REFERENCES

1. Lonhienne, T., Gerday, C., and Feller, G. (2000) *Biochim. Biophys. Acta* **1543,** 1–10
2. Feller, G., and Gerday, C. (1997) *CMLS Cell. Mol. Life Sci.* **53,** 830–841
3. Fields, P. A., and Somero, G. N. (1998) *Proc. Natl. Acad. Sci. U. S. A.* **95,** 11476–11481
4. Hochachka, P. W., and Somero, G. N. (1984) *Biochemical Adaptations*, pp. 355–449, Princeton University Press, Princeton, NJ
5. Georlette, D., Damien, B., Blaise, V., Depiereux, E., Uversky, V. N., Gerday, C., and Feller, G. (2003) *J. Biol. Chem.* **278,** 37015–37023
6. Georlette, D., Blaise, V., Collins, T., D'Amico, S., Gratia, E., Hoyoux, A., Marx, J. C., Sonan, G., Feller, G., and Gerday, C. (2004) *FEMS Microbiol. Rev.* **28,** 25–42
7. Miyazaki, K., Wintrode, P. L., Grayling, R. A., Rubingh, D. N., and Arnold, F. H. (2000) *J. Mol. Biol.* **297,** 1015–1026
8. Smalås, A. O., Leiros, H. K. S., Os, V., and Willassen, N. P. (2000) *Biotechnology Annual Review*, Vol. 6, pp. 1–57, Elsevier Science B.V., Amsterdam
9. Gerday, C., Aittaleb, M., Bentahir, M., Chessa, J. P., Claverie, P., Collins, T., D'Amico, S., Dumont, J., Garsoux, G., Georlette, D., Hoyoux, A., Lonhienne, T., Meuwis, M. A., and Feller, G. (2000) *Trends Biotechnol.* **18,** 103–107
10. Russell, R. J. M., Gerike, U., Danson, M. J., Hough, D. W., and Taylor, G. L. (1998) *Structure* **6,** 351–361
11. Brandsdal, B. O., Smalås, A. O., and Åqvist, J. (2001) *FEBS Lett.* **499,** 171–175
12. Moe, E., Leiros, I., Riise, E. K., Olufsen, M., Lanes, O., Smalas, A., and Willassen, N. P. (2004) *J. Mol. Biol.* **343,** 1221–1230
13. Lindahl, T., and Nyberg, B. (1974) *Biochemistry* **13,** 3405–3410
14. Mol, C. D., Arvai, A. S., Slupphaug, G., Kavli, B., Alseth, I., Krokan, H. E., and Tainer, J. A. (1995) *Cell* **80,** 869–878
15. Leiros, I., Moe, E., Lanes, O., Smalås, A. O., and Willassen, N. P. (2003) *Acta Crystallogr. Sect. D Biol. Crystallogr.* **59,** 1357–1365
16. Savva, R., Mcauleyhecht, K., Brown, T., and Pearl, L. (1995) *Nature* **373,** 487–493
17. Ravishankar, R., Sagar, M. B., Roy, S., Purnapatre, K., Handa, P., Varshney, U., and Vijayan, M. (1998) *Nucleic Acids Res.* **26,** 4880–4887
18. Slupphaug, G., Mol, C. D., Kavli, B., Arvai, A. S., Krokan, H. E., and Tainer, J. A. (1996) *Nature* **384,** 87–92
19. Parikh, S. S., Walcher, G., Jones, G. D., Slupphaug, G., Krokan, H. E., Blackburn, G. M., and Tainer, J. A. (2000) *Proc. Natl. Acad. Sci. U. S. A.* **97,** 5083–5088
20. Parikh, S. S., Mol, C. D., Slupphaug, G., Bharati, S., Krokan, H. E., and Tainer, J. A. (1998) *EMBO J.* **17,** 5214–5226
21. Bianchet, M. A., Seiple, L. A., Jiang, Y. L., Ichikawa, Y., Amzel, L. M., and Stivers, J. T. (2003) *Biochemistry* **42,** 12455–12460
22. Lanes, O., Leiros, I., Smalås, A. O., and Willassen, N. P. (2002) *Extremophiles* **6,** 73–86
23. Lanes, O., Guddal, P. H., Gjellesvik, D. R., and Willassen, N. P. (2000) *Comp. Biochem. Physiol.* **127,** 399–410
24. Leiros, I., Lanes, O., Sundheim, O., Helland, R., Smalås, A. O., and Willassen, N. P. (2001) *Acta Crystallogr. Sect. D Biol. Crystallogr.* **57,** 1706–1708
25. Jones, T. A., Zou, J. Y., Cowan, S. W., and Kjeldgaard, M. (1991) *Acta Crystallogr. Sect. A* **47,** 110–119
26. Dinner, A. R., Blackburn, G. M., and Karplus, M. (2001) *Nature* **413,** 752–755
27. Pearlman, D. A., Case, D. A., Caldwell, J. W., Ross, W. S., Cheatham, T. E., Debolt, S., Ferguson, D., Seibel, G., and Kollman, P. (1995) *Comp. Phys. Commun.* **91,** 1–41
28. Cornell, W. D., Cieplak, P., Bayly, C. I., Gould, I. R., Merz, K. M., Ferguson, D. M., Spellmeyer, D. C., Fox, T., Caldwell, J. W., and Kollman, P. A. (1995) *J. Am. Chem. Soc.* **117,** 5179–5197
29. Berendsen, H. J. C., Postma, J. P. M., Vangunsteren, W. F., Dinola, A., and Haak, J. R. (1984) *J. Chem. Phys.* **81,** 3684–3690
30. Darden, T., York, D., and Pedersen, L. (1993) *J. Chem. Phys.* **98,** 10089–10092
31. Ryckaert, J. P., Ciccotti, G., and Berendsen, H. J. C. (1977) *J. Comp. Phys.* **23,** 327–341
32. Jorgensen, W. L., Chandrasekhar, J., Madura, J. D., Impey, R. W., and Klein, M. L. (1983) *J. Chem. Phys.* **79,** 926–935
33. Merritt, E. A., and Bacon, D. J. (1997) *Methods Enzymol.* **277,**
34. Kabsch, W., and Sander, C. (1983) *Biopolymers* **22,** 2577–2637
35. Kraulis, P. J. (1991) *J. Appl. Crystallogr.* **24,** 946–950